Chapter

OCT for Examination of Cultural Heritage Objects

Piotr Targowski, Magdalena Kowalska,
Marcin Sylwestrzak and Magdalena Iwanicka

Abstract

Optical coherence tomography (OCT) was first time reported as a tool for examination of cultural heritage objects in 2004. It is mainly used for the examination of subsurface structure of easel paintings (such as varnishes and glazes) and has also been successfully used for inspection of other types of artworks, provided that they contain layers that are permeable to the probing light. This chapter discusses the last applications of OCT in this area with an emphasis on synergy with some other noninvasive techniques such as large-scale X-ray fluorescence (XRF) scanning and reflective Fourier transform infrared (FTIR) spectroscopy. After this part, there is a detailed description of the high-resolution OCT instrument developed by the authors specifically for the study of works of art. Next, two examples are given for the structural examination of works of art: in the former, the subsurface layers of an easel painting are presented, and in the latter, the painting on reverse of the glass is examined, when the inspection must be carried out through the glass. Finally, an application for the assessment of chemical varnish removal from an easel panel painting is discussed in details.

Keywords: artwork, painting, varnish, heritage science, cleaning of paintings

1. Introduction

Optical coherence tomography is a quite natural choice for examination of objects of art. This is because it is possible to make it portable and it is contactless and noninvasive. As for the former, it is significant that the distance to an examined object is usually relatively high—in a range of centimeters rather than millimeters. It is especially important for the fragile pieces of art examined in situ, with the portable instrument mounted on a tripod or similar provisional stand. As for the latter, the intensity of the probing radiation and low energy of infrared protons ensure lack of physicochemical damage to any material: let us consider an instrument with the power of the probing beam at the object of 1 mW. If the Fourier domain fast OCT system is considered, it is reasonable to assume that the 15-mm wide B-scan is acquired in less than 0.1 s and composed of, let us say, 3000 A-scans. It leads to the scanning speed over 150 mm/s and 33 μs/A-scan. If the spot diameter will be about 12 μm, what is a reasonable measure of the lateral resolution, the fluence of the OCT beam can be estimated at 30 mJ/cm^2. This quantity is far below any damage thresholds for long pulses of infrared radiation, but a certain care in the case of work with photosensitive objects must be adopted [1].

2. An overview of recent applications of OCT in heritage science

The noninvasiveness of OCT encouraged heritage science researches to seek its applications to examination of objects of art. This subject is present in the literature since 2003 when first reports appeared [2–5]. The major fields of application have been, from the very beginning, examination of subsurface, semitransparent layers of easel paintings, glazes at faience and ceramics, historic glass, jade, and occasionally some other materials. The main restriction is in limited transparency to the probing light of materials constituting those objects. This issue has been a subject of detailed examination by Liang et al. [6] in search for the optimum wavelength window for examination. As expected the mid-IR band, about 2 μm, was found as more suitable from the point of view of transparency of pigments and dyes usually present in easel paintings. However, OCT instruments (at least commonly available) working in this range exhibit lower axial resolution due to the known trade-off between resolution and the central wavelength of operation. Nevertheless, the bibliography [7] of the subject counts now over 130 positions which is a negligible amount in comparison to those dedicated to medical applications, but constituting a little community of researchers permanently devoted to this subject. The subject has been reviewed twice already [8, 9], so for the rest of this chapter, only some of the last reports (published after 2014) will be commented on. For the complete bibliography, the reader is directed to the aforementioned website.

As for the further development of the technique, a paper by Cheung et al. [10] may serve as a mature example of the system working in 800 nm band and taking a full advantage of the axial resolution available in the near-infrared range. Due to the careful design and very broad light source (with FWHM of ∼200 nm after shaping to Gaussian-like function), the axial resolution of 1.8 μm (1.2 μm in varnish-like medium of n_R = 1.5) is reported. The system permits resolving varnish layers as thick as 2–6 μm what is sufficient for most of examinations of easel paintings. Unfortunately, this was not a case with the second system [11] reported by the same group: the use of the supercontinuum source with the bandwidth of 220 nm working in the 2 μm range resulted in very good transparency of many layers, not permeable in 900 nm band, but the measured axial resolution was 13 μm in air which may not be sufficient for some applications.

Numerical post-processing of the results is one of the most decisive factors of the advance applications, going beyond simple feasibility studies. Usually, the solutions are adopted from the medical applications, and some concepts developed in our laboratory will be mentioned in the next sections. Here we would like to refer the reader to the paper by Callewaert et al. [12] devoted to the important subject of segmentation of thin layers, leading to, e.g., at least semiautomatic determination of thickness of superficial structures like varnish layers. This may pave the way to more efficient, or even fully automatic, monitoring of some restoration processes, even with the use of laser ablation of unwanted layers.

The area of applications of OCT to heritage objects is still expanding. Over the last few years, reports on the novel use of OCT for rock vulnerability assessment [13] and protective coatings on metal [14] have emerged. Moreover, recently the combined use of OCT with some other techniques, to take advantage of the synergy effect, has been reported. It is a known deficiency of the OCT that it does not provide information on chemical composition of structures visualized. To overcome this problem, it may be combined with other techniques, sensitive to the composition of the object, but lacking an in-depth resolution. The most promising solution seems to be linking OCT with X-ray fluorescence (XRF), especially with its

macro-imaging modality MA-XRF. This combination has been presented in application for examination of the seventeenth-century Dutch still life painting [15, 16] —namely, to localize within the structure of paint layers the presence of zinc white and to clearly associate it with overpaintings present due to former restoration attempt and not with the original structures. It was important for dating of the painting since zinc white had been in common use since the second quarter of the nineteenth century only [17] and therefore, if present in the original paint layer, would shift the attribution and dating of the painting toward modern times. As for the application of MA-XRF and OCT to other kinds of artworks, in case of the late sixteenth-century illuminated manuscript (the gradual) [18], the initials made with cobalt glass pigment (smalt) and text written with iron-gall ink were in focus of the research and were well visualized by means of both OCT and MA-XRF. Another imaging technique used in combination with OCT is multispectral infrared reflectography. It permits inspection of the object in different wavelength ranges, beyond the OCT probing light [19–21]. The concept of expanding the examination window even further lies at the foundations of the complementary use of OCT and terahertz time domain imaging presented by Koch Dandolo et al. [22]. This preliminary test has shown that, as expected, the THz imaging overcomes the major limitation of OCT caused by the limited permeability of paint layer and allows imaging down to the canvas support. However, there are two other factors, which restrict the use of the THz imaging alone: the limited contrast sometimes impairs the ability to differentiate various structures (e.g., varnish versus paint) and the axial resolution, about tenfold lower than in the case of OCT. All this especially predesignate these techniques for complementary use.

The capabilities of the common use of OCT and nonlinear microscopy (NLM) were investigated by Liang et al. [1]. It was shown that NLM may in some cases provide a better contrast to differentiate between varnishes. On the other hand, this technique must be applied with care, to avoid light-induced damage of especially light-sensitive objects.

The holistic approach, including VIS-NIR multispectral imaging, high-spectral resolution VIS-NIR spectroscopy with fiber-optic reflectance spectroscopy (FORS), micro-Raman spectroscopy, XRF spectroscopy, and OCT imaging, was used by Kogou et al. [23] for examination of Chinese watercolors. In this case OCT could have been utilized as a complementary tool only, since watercolors do not exhibit permeable layers possible to examine with OCT. Therefore, it was applied in order to investigate a structure of supporting papers. Even though these materials are also essentially not permeable, some conclusions were possible to be drawn.

Properties of coatings on wood were intensively investigated lately with optical coherence microscopy exclusively [24], with OCT and hyperspectral imaging [25], as well as with OCT and synchrotron radiation micro-computed tomography (Sr-micro-CT) [26]. In this last case, the subject of examination was five large fragments removed during past restorations from historic string instruments produced by famous Italian historical violin makers: Jacobus Stainer, Gasparo da Salò, Giovanni Paolo Maggini, and Lorenzo Guadagnini. This research may be considered as feasibility study for planned examination of historic violins and showed a significant complementarity of both tomographic approaches. SR-micro-CT has better axial resolution enabling imaging some thin varnish layers, but in some cases, OCT provides better contrast permitting identification of a thin preparation layer spread over the wood, not seen with micro-CT.

The development of the OCT technique as a whole over the last 15 years as well as its applications to the examination of cultural heritage objects has permitted resolving of specific conservation issues, posted by art restorers and objects' curators.

Preceding the restoration campaign, performed in Opificio delle Pietre Dure in Florence, the unfinished masterpiece by Leonardo da Vinci "Adoration of the Magi" was extensively examined with various techniques. Among others, OCT was used [27] to determine the condition and structure of secondary varnish layers covering the painting.

OCT examination is especially effective when it is used in combination with other techniques. One of the first holistic attempts was examination of the "Bessarion Reliquary" at Opificio delle Pietre Dure in 2012 [28]. The research was directed toward the understanding of the character of specific damages of the varnish covering the painted parts of the object and tracing of remains of the historical restoration commissioned by cardinal Bessarion in the fifteenth century. Apart from OCT also point-wise XRF examination was used. Additionally, on samples collected from the object, gas chromatography with mass spectroscopy detection (GC-MS), pyrolysis gas chromatography with mass spectroscopy detection (PGC-MS), scanning electron microscopy with energy dispersive spectroscopy (SEM-EDS), and Fourier transform infrared (FTIR) spectroscopy techniques were used. Consequently, the results had been used for planning of the restoration campaign (already completed).

The combination of SEM and SEM-EDS with OCT was used by Yang et al. [29] to investigate optical properties and structure of Chinese Song Jun glaze on porcelain, especially the presence of copper and quartz additives.

During the same examination campaign as for the "Adoration of the Magi," another painting by Leonardo and studio was examined: "The Lansdowne Virgin of the Yarnwinder" ("Madonna dei Fusi"). The results of its investigation with OCT, multispectral scanning, and more common techniques, X-radiography and UV-excited fluorescence, were published recently [21]. Data post-processing with the innovative generation of scattering maps from a given depth under the surface clearly revealed the shape and in-depth location of vast overpaintings, not seen clearly with other, conventional techniques. Probably, these interventions were performed to hide damage created during two transfers of paint layer: from wood panel to canvas and from canvas to composite rigid support. The evidence of the first transfer canvas, not existing presently, was found with OCT examination as well in a form of an imprint in the paint layer. Another multi-instrumental examination campaign, the comprehensive study of Amsterdam version of "Sunflowers" by Vincent van Gogh at Van Gogh Museum in Amsterdam, was performed in 2016 as a transnational access MOLAB activity [30] of H2020 IPERION CH project. The research was aimed at documentation of a state of preservation, possible threats related to exposition, and resolving the history of restorations of this masterpiece. The goal of the OCT research was to determine the number and thickness of varnish layers and the stratigraphy within the restored areas. OCT was also used for examination of deterioration phenomena typical for this painting: local darkening of varnish in the recesses of the brush strokes, migration of the paint layer into the varnish, as well as presence and potential development of lead soap formations [31].

Apart from these reports, devoted to examination of the structure and state of preservation of artworks, OCT has been also used to monitor or assess some restoration treatments. One of the early reports, from 2011, was about application of OCT to real-time monitoring of consolidation of paint layer in reverse painting on glass (*Hinterglasmalerei*) objects [32].

Due to transparency of varnish layer, OCT is especially well suited to monitor its removal. The most common restoration technique used for this purpose is with the use of solvents. OCT, especially if used together with FTIR spectroscopy examination, is capable of accurate assessment of the cleaning process [33, 34]. Some tests of this kind were also performed during the aforementioned examination campaign of

van Gogh's "Sunflowers" [35]. Selected aspects of OCT data processing for this purpose will be addressed in Section 5.

The use of lasers for ablation of unwanted layers (such as varnishes or mineral deposits) from paintings and other objects is a particularly delicate operation which needs precise control. Feasibility studies presented at LACONA (Lasers in the Conservation of Artworks) conferences in 2007, 2013, and 2015 [36–38] proved that it is possible to efficiently monitor such a process in real time. A specific case of removal of unwanted layers from the substrates of mural paintings was addressed by Striova et al. firstly in the case of removal of shellac varnish [39] and then of calcium oxalate layers [40], in both cases by means of laser and chemical treatment.

3. OCT instrument designed for heritage science

3.1 Opto-mechanical details

The instrument, constructed especially for examination of cultural heritage objects and being developed permanently in our laboratory, belongs to Fourier domain category with a broadband source and a spectrograph as detector. The instrument is designed as a portable one. To achieve this, a modular design composed of easy detachable parts connected with cables and optical fibers was chosen. All elements are of weight allowing easy handling by one person. Only a computer, comprising also all high power suppliers, weighs about 30 kg. This is important because objects of arts are often localized in old buildings with a limited access.

As for the operating parameters, the highest available axial resolution was chosen as the key parameter. This is because the ability to distinguish and visualize thin layers is a decisive factor for using in this area of applications. Therefore, short-infrared radiation was chosen even though the transparency of typical pigments is limited in this area and the optimum wavelength range lays around 2 μm [41]. By using portable commercial sources composed of coupled superluminescent diodes (Broadlighters: Q-870-HP or M-T-850-HP-I both from Superlum, Ireland) emitting in the range 770–970 nm (the former) and 750–960 (the latter), it was possible to achieve 3.3 μm of (measured) axial resolution in air, and 2.2 μm in medium of $n_R = 1.5$. The resolution was measured as a width of the point spread function with sidelobes suppression better than 25 dB. This last condition is very important in the case of examination of CH objects since they are often composed of thin and clearly transparent layers. In this case sidelobes may be easy misinterpreted as an evidence of a thin, additional layer just under the surface.

After the source, light passes a fiber-optic polarization controller and an optical isolator and is transmitted to the second module—a head by the optical fiber. The head comprises a fiber coupler of the interferometer and its reference and object arms. The former is built of the collimator, light attenuator, dispersion compensator (LSM02DC from Thorlabs), and a mirror mounted on a small translation stage. The latter comprises a fiber-optic polarization controller, the identical collimator and attenuator as in the reference arm, galvanometric scanners (6220H galvanometer scanners with MicroMax HP servo driver amplifier from Cambridge Technology, USA), and the telecentric lens (LCM04 from Thorlabs, F = 54 mm).

This optical setup provides lateral resolution of 12 μm with the distance to the object from the most protruding element of the lens equal to 43 mm and maximum scanning area of $17 \times 17 \text{ mm}^2$. Alternatively the head can work with the LCM02 lens (F = 18 mm) that improves the lateral resolution to $6.5 \times 6.5 \text{ mm}^2$ but for the price of significantly smaller distance to the object, 7 mm, and scanning area, $5 \times 5 \text{ mm}^2$. A significant distance to the object is important for CH applications because it

increases the safety of operation—objects sometimes have an irregular shape, and manipulating the head very close to the surface may pose a danger of direct contact with the artwork.

The head is equipped with two HR CCD cameras with USB-2 interface for precise documentation of the location of the OCT scanning and precise step motor-driven translators to position the head in plane and to control the distance to the object.

Finally, the light reflected in the reference arm and returning from the object undergoes the interference in the abovementioned fiber coupler and is transferred by the optical fiber to the third module—a spectrograph. Initially, the laboratory-built device with volume-phase holographic transmission grating optimized for 850 nm and with 1200 grooves/mm from Wasatch Photonics was used. Lately, it has been replaced by the complete Cobra CS800-840/180 spectrometer from Wasatch Photonics in order to improve mechanical stability and roll-off performance. Both spectrographs use 2048 pixel linear CCD cameras with fast 4-tap CameraLink interface.

3.2 Data processing and software

In the case of Fourier domain OCT instruments utilizing spectrometers with linear cameras to collect interference spectra, the result is the vector of numbers of a length equal to the number of pixels of the camera (usually 2048). This data vector requires a set of numerical procedures to be converted into one axial line of the tomogram (A-scan). Over the time, by accumulating the common experience, a standard set of numerical procedures required to obtain a high-quality A-scan has been established. It comprises a sequence of six steps: background (BG) subtraction (labelled as 1 in Figure 1), λ-k remapping (2), numerical dispersion compensation (3), spectral shaping (4), fast Fourier transformation (FFT - 5), and finally displaying in logarithmic scale (6). No one of these steps may be omitted if the best available quality of results is expected. The influence of each of the abovementioned procedures on the cross-sectional image (B-scan) is presented in **Figure 1**: a completely illegible tomogram obtained only by executing the Fourier transform on recorded spectra and displayed in logarithmic scale is presented in **Figure 1a**. The next panels show the effect of the background (BG) subtraction procedure (**Figure 1b**) and remapping of the interference spectrum from the wavelength λ (or just a camera) domain to the wavenumber k domain (**Figure 1c**). Numerical dispersion compensation (**Figure 1d**) is sharpening the image by compensating the residual dispersion mismatch between both arms of the interferometer. It is especially useful when data is collected from the structures located deep in the object of high dispersion. For example, it is a case when measurement is performed though thick glass sheet covering the investigated structures of the artwork (see **Figure 3** in the next chapter). Spectral shaping completes the set of procedures (**Figure 1e**), improving the sharpness of the boundaries of imaged structures by minimizing the sidelobes generated in the optical A-scan as a result of the Fourier transformation of the signal of the non-Gaussian envelope. This operation, being essentially the windowing of the data, may—however—slightly reduce the resolution of the system.

In order to obtain the resultant tomogram (B-scan) of the best quality, the whole set of numerical procedures presented above must be performed for every spectrum. Assuming earlier preparation of the necessary data common for all spectra (in particular vectors used in procedures of numerical dispersion compensation and λ-k remapping [42]), this analysis does not require complicated calculations: BG subtraction needs calculation of the difference of two vectors (2048 elements each); dispersion compensation and shaping are just multiplications by vectors—element
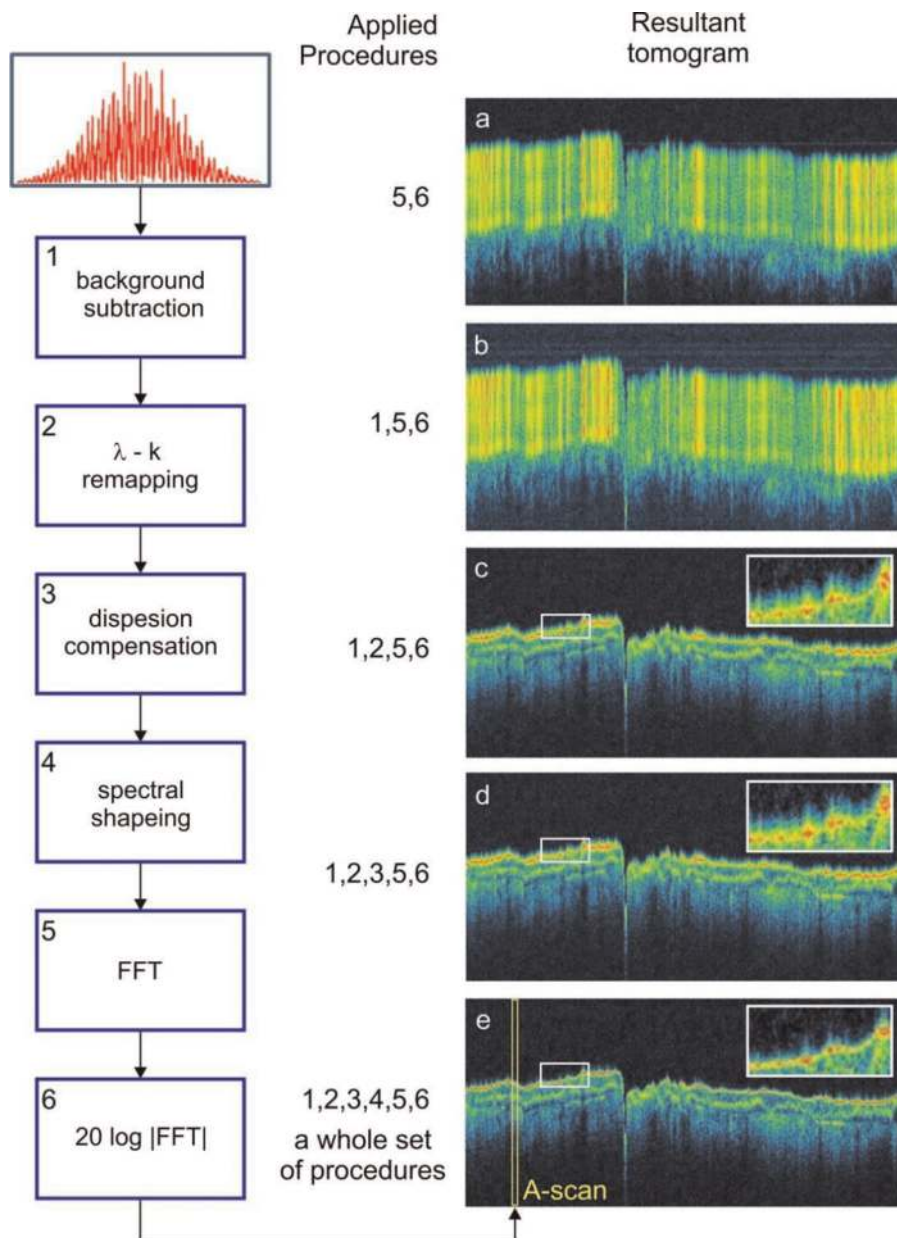
Figure 1.
The impact of individual numerical procedures on the quality of the OCT tomogram applied to a single A-scan. The procedures are labelled with numbers 1..6 and described in the text. False color scale is applied.

by element. FFT calculations are very well implemented and optimized in public domain libraries and do not take much time. λ-k remapping needs interpolation of the data (fourfold in our system, performed in Fourier domain, two FFT required) and mapping onto 2048 elements vector by a linear interpolation. The complexity of this problem arises with the number of A-scans, which must be processed—in the case of 3D volume analysis, this number typically exceeds 300,000.

Graphic processor units (GPU) are systems initially designed for fast rendering of graphic data by parallel calculations, but at present the area of applications is much broader. Often the visualization is not the major task but the massively parallel processing of any data. Obviously not all algorithms are appropriate for implementation and run fast on the GPU. However, if there is a possibility of parallelization of certain numerical tasks, the efficiency of calculations increases with the amount of data processed. In this context, the analysis of spectral optical

	Task	Time [ms] Intel Core i7-7700K GTX 1080		Time [ms] Intel Core i7-960 GTX 580	
GPU	Transfer data to the GPU	5.77	15.27	7.45	24.36
	Processing	6.86		13.20	
	Transfer of the results to the host	2.64		3.71	
CPU	Processing	940		1200	
CPU/GPU time		62		49	

Table 1.
The time profit of using GPU processing over using the main processor (CPU) measured for two systems: modern, with Intel Core i7-7700K and actually installed in our tomograph, with Intel Core i7-960.

tomography data is well suited for parallelization using the GPUs—calculations performed on successive spectra are independent of each other, and the complexity is primarily related to the amount of data being processed.

To benefit from this advantage of GPU, we have developed and successfully implemented our own software for parallel processing of the OCT data [43, 44]. It is worthwhile to note that in the case of this implementation, more time is needed to transfer the raw data to the GPU memory, and, after processing, the results back to the RAM memory of the workstation through the PCIe bus (**Table 1**). Nevertheless the profit of fast calculations is so high that the implementation of GPU is fully justified.

The efficiency of this data processing depends on the utilized hardware. On a modern workstation equipped with an Intel Core i7-7700K 4.2 GHz processor, 32 GB RAM memory, and NVIDIA GTX 1080 graphics processor, the computation acceleration is over 60 times when the process includes data transferring and almost 140 times for data processing only. The workstation actually used with our OCT configuration is equipped with Intel Core i7-960 3.2 GHz processors, 12 GB RAM, and NVIDIA GTX 580 GPU. The acceleration obtained with our software on this machine is slightly lower and amounts to 49 and 90 times (with and without data transfer). The details are presented in **Table 1**.

4. Examples of structural images of artwork

As a first example of application, OCT scans from examination of the early nineteenth-century painting on canvas "Portrait of Sir John Wylie" by F. Franck are presented (**Figure 2**). They are shown (as all tomograms in this chapter) with false color scale: structures strongly reflecting/scattering of the probing light are displayed in warm colors (red to yellow), whereas structures scattering/reflecting moderately or weekly in cold colors, from green to blue. Areas fully transparent or not accessible to the probing light are shown as black. The tomograms are corrected for refraction in the materials penetrated by the probing beam. Since most varnishes and binders have refractive indices from the range of 1.48 to 1.53 [45, 46], it is reasonable to assume an average value of 1.5 for recalculation of axial distances from optical to geometrical ones: for thin layers of varnishes possible systematic error will be below the axial resolution. The correction can be done either by the appropriate redrawing of the tomogram by application of a ray-tracing procedure taking into account ray refraction at the air-varnish boundary or by a simplified method. This approach, used in the examples presented herein, is acceptable for flat structures and is performed just by shortening of all vertical distances below the surface by a factor of 1.5. Alternatively, for uncorrected tomograms all axial optical
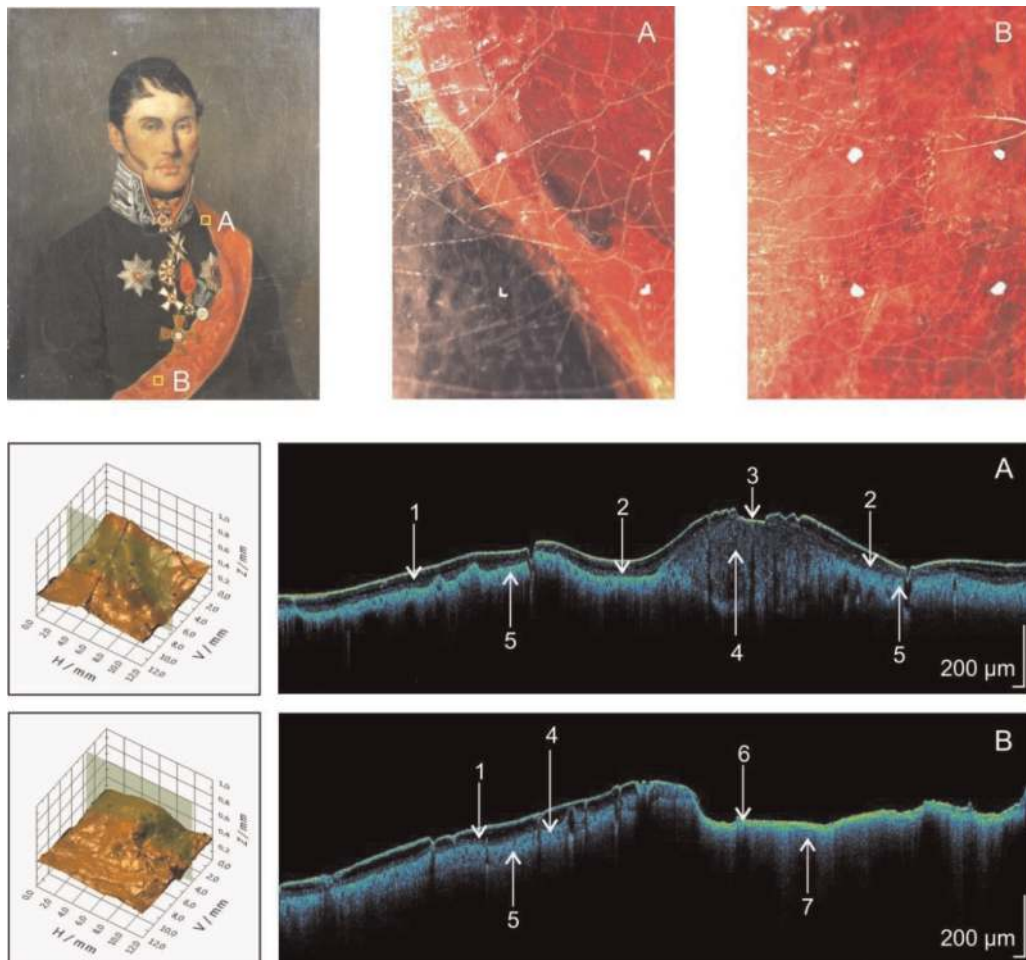
Figure 2.
OCT cross section over subsurface structures of an early nineteenth-century oil painting on canvas "Portrait of Sir John Wylie" by F. Franck. Tomograms (A, original structure of paint layers; B, restored structure at right) are corrected for refraction; thus, scale bars show geometrical distances, and false color intensity scale is used. Upper panels, from the left: a photo of the paintings with two spots (12 × 12 mm²) of examination marked as A and B, images from the OCT annotation camera with areas of OCT scanning clearly marked. Below: exemplary tomograms and surface profiles rendered for OCT data with exact locations of OCT scans marked green. Tomograms and surface profiles are vertically stretched for better readability. Structures resolved: 1, three layers of varnish; 2, glaze layer; 3, loss in the varnish layer; 4, semitransparent paint layer; 5, opaque paint layer; 6, retouching covered by thin varnish layer; 7, putty.

distances below the surface and measured with scale appropriate for air above the object's surface (and thus for the surface topography) must be divided by 1.5. Another typical feature of tomograms used for this application is that they are vertically stretched for better readability. It is acceptable since the axial resolution is usually significantly higher.

In **Figure 2**, two examples are shown: (A) with original structure of paint layer and some secondary varnish layers and (B) area with original structure (left) and after considerable restoration (right) which included filing a paint loss with putty and reconstruction of the paint layer. Under surface of the painting, three varnish layers are seen and below, locally, a glaze layer. The last visible structure is always an opaque paint layer. If its absorption of OCT probing light is not extremely high, some multiscattering events within this layer occur, and fading tails of the signal are visible below the surface of paint (marked 5 and 7 in **Figure 2**).

Since OCT utilizes light to probe the object, it is possible to examine structures normally not accessible for inspection. As for the application to objects of art, it is

often the case of reverse paintings on glass (*la peinture sur verre inversé*, *Hinterglasmalerei*) technique popular in Europe, especially favored since the middle of the eighteenth century. Later, in the nineteenth century, it has become popular in folk art, especially in Central Europe. The picture is painted on glass and intended to be viewed through it. Glass serves both as the support and the protection of the paint, which makes this technique suitable for items designed for continuous use, such as decorations of craftwork, miniatures, devotional items, etc. The major disadvantage inherent for this painting technique is an overtime decrease of adhesion of the paint layer to glass, causing delamination. Ironically, the protecting glass complicates significantly the conservation treatments since the paint layer is not accessible from the front and very often also from the back.

OCT provides in this case a convenient method for examination of the state of preservation of the object. The application to folk art was reported already [47]; here it is demonstrated for the miniature from the collection of the National Museum in Krakow, Poland (**Figure 3**). The tomogram was collected through the
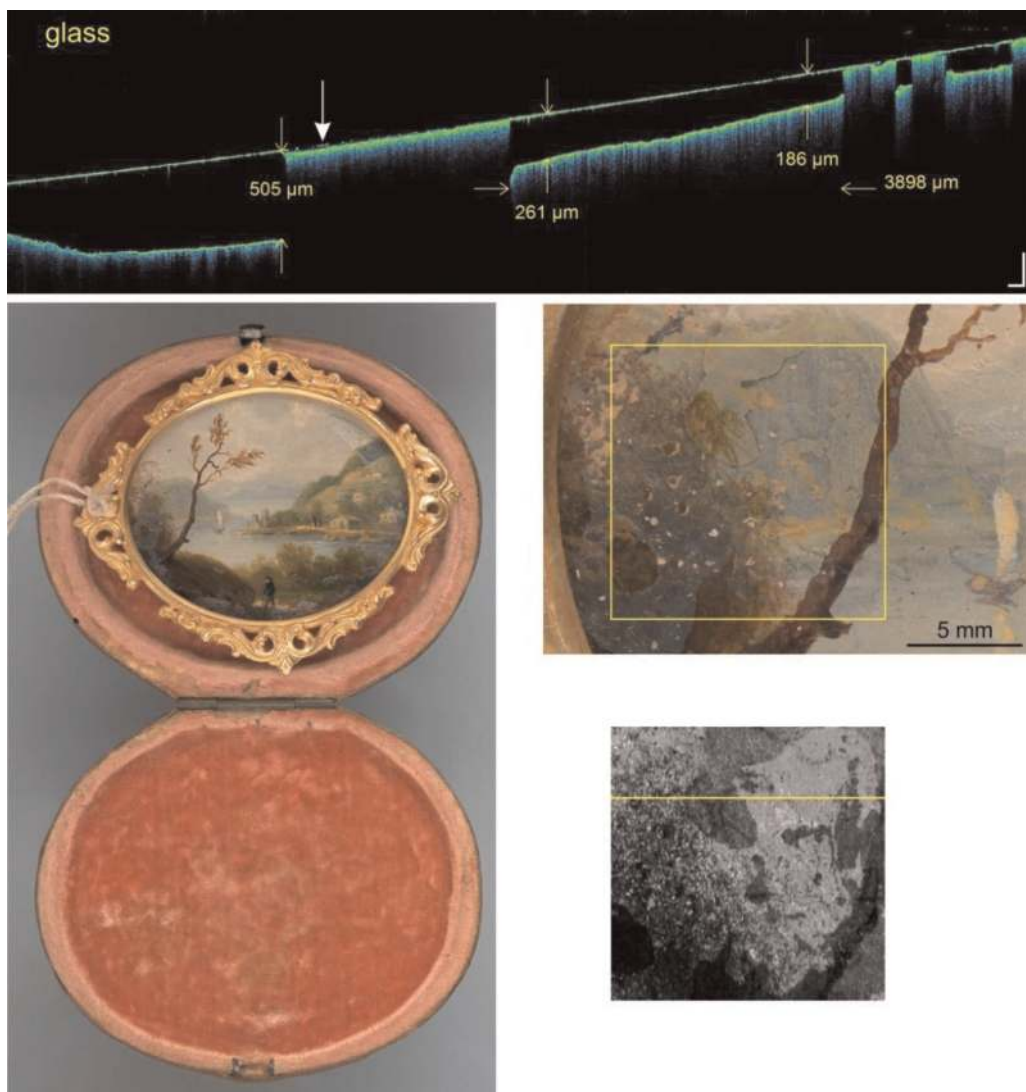
Figure 3.
Through glass OCT examination of the miniature from the collection of the National Museum in Krakow (MNK III-min 933), 5.2 × 6.3 cm², reverse paintings on glass. Tomogram is not corrected for refraction; scale bars represent 200 μm in both directions. White arrow points to the early delamination of paint. Photos: Karol Kowalik, Photographic Laboratory of National Museum in Krakow, PL. Bottom right. An IR reflectogram generated from OCT data by integration over A-scans with exact localization of the tomogram.

covering glass, and thus, its upper surface is not visible since it lies beyond the imaging range of the tomograph. Therefore, the first visible line from the top is a bottom surface of glass. Below, partially attached to the support, the paint layer is evident. The gap between glass and paint may be directly measured at the tomogram and in this case varies 0.19–0.26 mm for one flake and reaches even 0.5 mm for the other one. Additionally, some traces of further delamination (marked by white arrow) are discernible. It may be interpreted as an evidence of a progressing process of destruction.

5. Application for varnish removal assessment

Varnish removal is one of the most often performed restoration treatments. Despite the fact that according to the contemporary approach to conservation/restoration of artworks, interventions should be as minimal as possible, and removal of past varnishes is a commonly accepted practice. Most common reasons for this include yellowing of varnish changing the esthetic perception of the colors of the underlying paint as well as loss of varnish transparency due to its blanching, cracking, or delaminations. The action must be taken with caution so as not to damage the paint layer underneath. In particular, if most common chemical removal is planned, a proper solvent and means of use (through controlled swabbing or gel application) must be determined.

The ability of OCT to visualize varnish layers makes it a convenient tool to monitor a varnish removal with chemical treatment and/or laser ablation qualitatively [36, 37] and quantitatively [33, 39, 40]. An application of OCT for quantitative assessment of varnish removal by swabbing is experimentally challenging because it is difficult to avoid micro-displacements of the object between sequential measurements caused by the contact with a cotton swab. The amount of material removed in one step of swabbing (or other cleaning process, e.g., laser ablation) is measured by subtraction of two surface profiles, obtained before and after treatment. However, the result will be reliable only if the position of the object in 3D space before and after is the same with a micrometer precision. As it was mentioned earlier, it is usually not possible to mechanically maintain the position of the object with the required accuracy (especially in case of paintings on canvas). Therefore, one of OCT data set must be numerically shifted in all three dimensions to achieve desired correlation of surface profiles. If the cleaning spot is significantly smaller than the area covered by OCT 3D scan, the solution is quite simple: the requested shifts may be obtained by correlating the non-treated edges of the scanned area which—in this case—will be exactly the same [33]. If, however, for any reason, the surface of the whole scanned area was altered, another procedure must be applied. In order to determine the amount of the removed material, only surface profiles obtained from OCT data are needed. However, for the proper correlation of data cubes, the inner structure—obviously not altered by the treatment—must be used. In this case it is the surface of the opaque paint layer, well visible at the tomograms. To use it as a reference, however, the tomograms must be corrected for refraction: a thickness of varnish above is by definition different, and thus, the refraction deformation is different as well, and thus, correlation of images would be systematically wrong without such a correction.

In **Figure 4** the entire procedure is illustrated on the example of a multistep test of secondary varnish removal from a panel painting. In this case, the solvent treatment by means of swabbing was chosen. In every step a cotton swab with solvent was rolled over the surface of the painting once. The aim of the test was to determine a safe amount of rolls which will not affect a paint layer and assay the homogeneity of the treatment. Before the test and after each of 13 cleaning steps, a
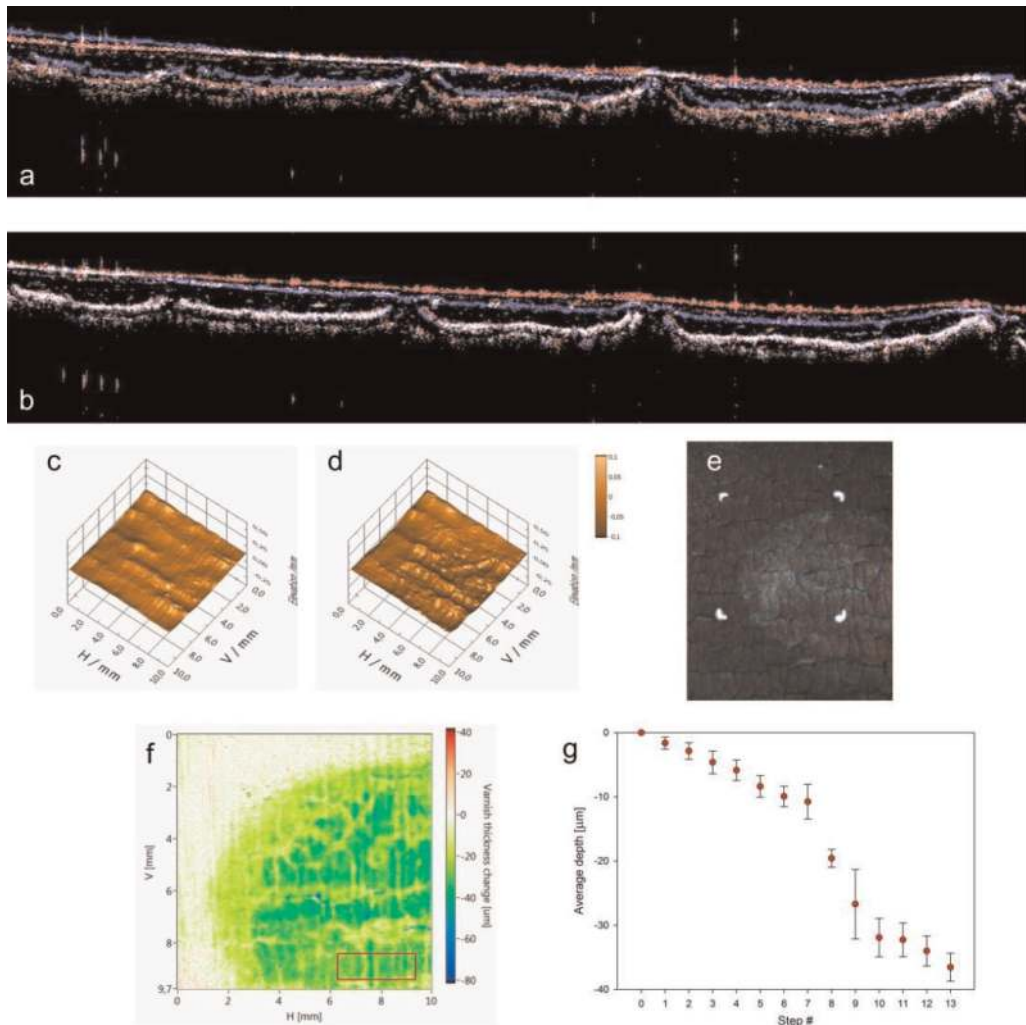
Figure 4.
Varnish removal monitoring by OCT; (a) superimposed OCT tomograms collected before (red) and after (blue) the 13th step of cleaning process, white dots represent pixels common in both tomograms, data not correlated, both tomograms corrected for refraction; (b) same but after correlation of the paint layer ($\Delta X = -30$, $\Delta Z = -13$ pixels); (c) surface profile before cleaning; (d) surface profile after cleaning; (e) photo from the OCT annotation camera taken after cleaning; (f) map of the varnish deficit after cleaning, red, area for averaging of varnish deficit; (g) average varnish thickness removed in consecutive steps.

3D OCT scan was performed over an area of 10×10 mm^2 by collection of 100 tomograms composed of 3000 A-scans each. Exemplary tomograms, chosen only for presentation in this account, are shown for all steps in Video 1 available from h ttp://repozytorium.umk.pl/handle/item/5906. Tomograms are not corrected for refraction; therefore, two scale bars are shown: for use in air and in a medium with $n_R = 1.5$. Random shifts both in X and Z directions are clearly visible. To process, at first the surface profiles were determined from each OCT 3D scan (see **Figure 4c** and **d** for two examples—before the test and after the last step, respectively). Then all OCT tomograms were corrected for refraction ($n_R = 1.5$) with simplified method as described above. As it can be seen from the exemplary tomograms (again before the test and after the last step) shown in **Figure 4a**, voxels are displaced in both X and Z directions due to unavoidable micro-displacements of the panel caused by contact with the swab. Therefore, the second tomogram had to be shifted in both directions to achieve desirable correlation of the paint layer (**Figure 4b**). It is worthwhile to note that in this particular case, displacement in Y direction, between B-scans, was determined to be smaller than the distance between adjacent scans

(0.1 mm) and thus was not taken into account. Knowing the necessary shifts, the maps of an amount varnish removed (deficit) were calculated (**Figure 4f**). For every map, the average amount was calculated over the red rectangle, and result is shown in **Figure 4g**. Since, for obvious reason, it is not possible to present in the figure results for all the steps, they can be viewed as Video 2 available from http://re pozytorium.umk.pl/handle/item/5905.

Inspection of results obtained with OCT from this test permits to draw certain conclusions important for planning of the prospective restoration. Firstly, the varnish removal is not homogenous: after 13 steps it is almost completely removed from most protruding areas at the raised edges of paint layer along craquelure (fully covered by varnish before treatment), whereas it remains in about ½ of it its original thickness in recesses. Surprisingly, as it can be clearly seen from **Figure 4**, the mechanical action (during swabbing) has less impact in the raised areas along the craquelure than in the recesses. Apparently, the varnish is less soluble over the craquelure than in between. What is more, the analysis of **Figure 4g** leads to the conclusion that there is a critical range in the process around the eighth step, when it develops very quickly and the thickness of the varnish decreases rapidly. This is due to the phenomenon of swelling of varnish. Knowing at which point in the cleaning process this rapid leap in the varnish removal rate occurs aids the conservator-restorer to control the process with caution. In the case of the painting presented here, the varnish removal rate decreased in the last four steps of the OCT-monitored cleaning test. The reason for this is uncertain, one may hypothesize that the bottom varnish layers were less soluble since they were the oldest ones.

Such monitoring of the dynamic of varnish removal with OCT, even if performer locally, can then be utilized by the restorer to safely clean the whole painting, now without OCT assistance.

6. Conclusions

OCT has been used to study works of art for the last 15 years. During this time, a set of applications was developed, related to the study of the structure of the artwork, especially as a supporting tool for preventive conservation and restoration. The ability of OCT to inspect superficial layers like varnishes, glazes, and overpaintings—just to use examination of easel paining as an example—makes it especially efficient in tracing former restorations and detecting surface-related damages such as cracks, delaminations, lead soap formations, etc. In many cases, especially for most valuable artworks as well as the ones in a good state of preser-vation without visible losses, traditional method of investigation of the structure of an object of art by taking samples of the material is not permitted. Due to its noninvasiveness, OCT is in this case the only technique capable of visualization of the subsurface structures of works of art with desirable resolution and contrast. The OCT examination is also fast and possible to be carried out in a place where the objects are stored or displayed. This last remark is, as it is clear from the experience of the authors, very important, because in the focus of all the curators of collections is the safety of objects and their preservation for future generations. There is no doubt that optical coherence tomography contributes to this goal.

Acknowledgements

of the Interdisciplinary Centre for Modern Technology of Nicolaus Copernicus University in Toruń, Poland, and financed by the Regional Operational Programme for Kujawsko-Pomorskie Voivodeship (Project No. RPKP.05.04.00-04-001/10). Results shown in **Figure 3** are obtained in cooperation with the National Museum in Krakow in the framework of the offer of the Polish Research Consortium for Heritage Science E-RIHS.PL (project leader: Zofia Maniakowska-Jazownik). A valuable contribution of Ms. Hélène Dubois from KIK-IRPA, Brussels, to conducting a cleaning test is gratefully acknowledged.

Conflict of interest

The authors declare no conflict of interest.

Author details

Piotr Targowski[1]*, Magdalena Kowalska[1], Marcin Sylwestrzak[1] and Magdalena Iwanicka[2]

1 Faculty of Physics, Astronomy and Informatics, Nicolaus Copernicus University, Toruń, Poland

2 Faculty of Fine Arts, Nicolaus Copernicus University, Toruń, Poland

*Address all correspondence to: ptarg@fizyka.umk.pl

IntechOpen

References

[1] Liang H, Mari M, Cheung CS, Kogou S, Johnson P, Filippidis G. Optical coherence tomography and non-linear microscopy for paintings—A study of the complementary capabilities and laser degradation effects. Optics Express. 2017;**25**(16):19640-19653. DOI: 10.1364/OE.25.019640

[2] Targowski P, Rouba B, Wojtkowski M, Kowalczyk A. Application of optical coherence tomography to non-destructive examination of museum objects. Studies in Conservation. 2004;**49**(2):107-114. DOI: 10.1179/sic.2004.49.2.107

[3] Yang ML, Lu CW, Hsu IJ, Yang CC. The use of optical coherence tomography for monitoring the subsurface morphologies of archaic jades. Archaeometry. 2004;**46**(2):171-182. DOI: 10.1111/j.1475-4754.2004.00151.x

[4] Arecchi FT, Bellini M, Corsi C, Fontana R, Materazzi M, Pezzati L, et al. Optical coherence tomography for painting diagnostics. Proceedings of SPIE. 2005;**5857**:58570Z-1-58570Z-5. DOI: 10.1117/12.612558

[5] Liang H, Gomez Cid M, Cucu R, Dobre G, Podoleanu A, Pedro J, et al. En-face optical coherence tomography—A novel application of non-invasive imaging to art conservation. Optics Express. 2005;**13**(16):6133-6144. DOI: 10.1364/OPEX.13.006133

[6] Cheung CS, Daniel JMO, Tokurakawa M, Clarkson WA, Liang H. Optical coherence tomography in the 2-μm wavelength regime for paint and other high opacity materials. Optics Letters. 2014;**39**(22):6509-6512. DOI: 10.1364/OL.39.006509

[7] Optical Coherence Tomography for Examination of Works of Art—A Complete List of Papers on Application of OCT to Examination of Artwork [Internet]. Available from: http://www.oct4art.eu [Accessed: 08 June 2019]

[8] Targowski P, Iwanicka M. Optical coherence tomography: Its role in the non-invasive structural examination and conservation of cultural heritage objects—A review. Applied Physics A: Materials Science & Processing. 2012;**106**(2):265-277. DOI: 10.1007/s00339-011-6687-3

[9] Targowski P, Iwanicka M, Rouba BJ, Frosinini C. OCT for examination of artwork. In: Drexler W, Fujimoto G, editors. Optical Coherence Tomography Technology and Applications. Cham Heidelberg New York Dordrecht London: Springer; 2015. pp. 2473-2495

[10] Cheung CS, Spring M, Liang H. Ultra-high resolution Fourier domain optical coherence tomography for old master paintings. Optics Express. 2015;**23**(8):10145-10157. DOI: 10.1364/OE.23.010145

[11] Cheung CS, Daniel JMO, Tokurakawa M, Clarkson WA, Liang H. High resolution Fourier domain optical coherence tomography in the 2 um wavelength range using a broadband supercontinuum source. Optics Express. 2015;**23**(3):1992-2001. DOI: 10.1364/oe.23.001992

[12] Callewaert T, Dik J, Kalkman J. Segmentation of thin corrugated layers in high-resolution OCT images. Optics Express. 2017;**25**(26):32816-32828. DOI: 10.1364/oe.25.032816

[13] Bemand E, Liang H, Bencsik M. Non-invasive methods for in-situ assessing and monitoring of the vulnerability of rock-art monuments. In: Darvill T, Batarda Fernandes AP, editors. Open-Air Rock-Art Conservation and Management: State of

the Art and Future Perspectives. Abingdon: Routledge; 2014. pp. 244-258

[14] Lenz M, Mazzon C, Dillmann C, Gerhardt NC, Welp H, Prange M, et al. Spectral domain optical coherence tomography for non-destructive testing of protection coatings on metal substrates. Applied Sciences. 2017;7:364. DOI: 10.3390/app7040364

[15] Iwanicka M, Ćwikliński Ł, Targowski P. Combined use of Optical Coherence Tomography and Macro-XRF Imaging for Non-invasive Evaluation of Past Alterations in 17th c. Dutch Painting. Jerusalem. 2016. Available from: http://art2016.isas.co.il/wp-content/uploads/sites/10/2017/03/Session-I-Minerals-Pigments-Dyes-3-Iwanicka.pdf [Accessed: 23 June 2019]

[16] Iwanicka M, Sylwestrzak M, Targowski P. Optical coherence tomography (OCT) for examination of artworks. In: Bastidas DM, Cano E, editors. Advanced Characterization Techniques, Diagnostic Tools and Evaluation Methods in Heritage Science. Cham: Springer International Publishing; 2018. pp. 49-59. DOI: 10.1007/978-3-319-75316-4_4

[17] Kuhn H, White Z. In: Feller RL, editor. Artists' Pigments, a Handbook of their History and Characteristics. Vol. 1. London: Archetype; 1997. pp. 169-186

[18] Targowski P, Pronobis-Gajdzis M, Surmak A, Iwanicka M, Kaszewska EA, Sylwestrzak M. The application of macro-X-ray fluorescence and optical coherence tomography for examination of parchment manuscripts. Studies in Conservation. 2015;**60**(Supplement 1): S167-SS77. DOI: 10.1179/0039363015Z.000000000221

[19] Liang H, Burgio L, Bailey K, Lucian A, Dilley C, Bellesia S, et al. Culture and trade through the prism of technical art history: A study of Chinese export paintings. Studies in Conservation.

2014;**59**(sup1):S96-SS9. DOI: 10.1179/204705814x13975704318272

[20] Striova J, Dal Fovo A, Fontani V, Barucci M, Pampaloni E, Raffaelli M, et al. Modern acrylic paints probed by optical coherence tomography and infrared reflectography. Microchemical Journal. 2018;**138**:65-71. DOI: 10.1016/j.microc.2017.12.027

[21] Targowski P, Iwanicka M, Sylwestrzak M, Frosinini C, Striova J, Fontana R. Using optical coherence tomography to reveal the hidden history of *"The Lansdowne Virgin of the Yarnwinder"* by Leonardo da Vinci and studio. Angewandte Chemie. 2018;**57**: 7396-7400. DOI: 10.1002/anie.201713356

[22] Koch Dandolo CL, Lopez M, Fukunaga K, Ueno Y, Pillay R, Giovannacci D, et al. Toward a multimodal fusion of layered cultural object images: Complementarity of optical coherence tomography and terahertz time-domain imaging in the heritage field. Applied Optics. 2019;**58**(5):1281-1290. DOI: 10.1364/ao.58.001281

[23] Kogou S, Lucian A, Bellesia S, Burgio L, Bailey K, Brooks C, et al. A holistic multimodal approach to the non-invasive analysis of watercolour paintings. Applied Physics A: Materials Science & Processing. 2015;**121**(3): 999-1014. DOI: 10.1007/s00339-015-9425-4

[24] Gurov I, Margaryants N, Zhukova E. Evaluation of art subjects implemented in the marquetry technique by the optical coherence microscopy method. Strain. 2018;**0**(0): e12304. DOI: 10.1111/str.12304

[25] Dingemans LM, PV M, Liu P, Adam AJL, Groves RM. Optical coherence tomography complemented by hyperspectral imaging for the study of protective wood coatings. Proceedings

of SPIE. 2015;**9527**:952708. DOI: 10.1117/12.2184716

[26] Fiocco G, Rovetta T, Invernizzi C, Albano M, Malagodi M, Licchelli M, et al. A micro-tomographic insight into the coating systems of historical bowed string instruments. Coatings. 2019;**9**(2): 81. DOI: 10.3390/coatings9020081

[27] Iwanicka M, Sylwestrzak M, Szkulmowska A, Targowski P. Pre-restoration condition of superficial layers of the adoration of the magi by Leonardo da Vinci as seen by optical coherence tomography. In: Ciatti M, Frosinini C, editors. Il restauro dell'Adorazione dei Magi di Leonardo La riscoperta di un capolavoro. Florence: Edifir; 2017. pp. 287-293

[28] Iwanicka M, Lanterna G, Lalli CG, Innocenti F, Sylwestrzak M, Targowski P. On the application of optical coherence tomography as a complimentary tool in an analysis of the 13th century byzantine Bessarion reliquary. Microchemical Journal. 2016; **125**:75-84. DOI: 10.1016/j. microc.2015.11.014

[29] Yang M-L, Katz JI, Barton J, Lai W-L, Jau-Ho J. Using optical coherence tomography to examine additives in Chinese song Jun glaze. Archaeometry. 2014;**57**(5):837-855. DOI: 10.1111/arcm.12125

[30] MOLAB (Mobile LABoratory)—Transnational access to facilities within IPERION CH project or E-RIHS ERIC. Available from: http://www.iperionch.eu/molab/or http://www.e-rihs.eu/access/ [Accessed 09 June 2019]

[31] van den Berg KJ, Hendriks E, Geldof M, de Groot S, van der Werf I, Miliani C, et al. Structure and chemical composition of the surface layers in the Amsterdam Sunflowers. In: Hendriks E, Vellekoop M, editors. Van Gogh's Sunflowers Illuminated Art Meets Science. Amsterdam: Amsterdam

University Press/Van Gogh Museum Amsterdam; 2019. pp. 159-173

[32] Iwanicka M, Kwiatkowska EA, Sylwestrzak M, Targowski P. Application of optical coherence tomography (OCT) for real time monitoring of consolidation of the paint layer in Hinterglasmalerei objects. Proceedings of SPIE. 2011;**8084**: 80840G. DOI: 10.1117/12.890398

[33] Iwanicka M, Moretti P, van Oudheusden S, Sylwestrzak M, Cartechini L, van den Berg KJ, et al. Complementary use of optical coherence tomography (OCT) and reflection FTIR spectroscopy for in-situ non-invasive monitoring of varnish removal from easel paintings. Microchemical Journal. 2018;**138**:7-18. DOI: 10.1016/j.microc.2017.12.016

[34] Moretti P, Iwanicka M, Melessanaki K, Dimitroulaki E, Kokkinaki O, Daugherty M, et al. Laser cleaning of paintings: In situ optimization of operative parameters through non-invasive assessment by Optical Coherence Tomography (OCT), reflection FT-IR spectroscopy and Laser Induced Fluorescence spectroscopy (LIF) measurements. Heritage Science. 2019;**7**: 44-55. DOI: 10.1186/s40494-019-0284-8

[35] Hendriks E, Geldof M, van den Berg KJ, Monico L, Miliani C, Moretti P, et al. Conservation of the Amsterdam Sunflowers: From past to future. In: Hendriks E, Vellekoop M, editors. Van Gogh's Sunflowers Illuminated Art Meets Science. Amsterdam: Amsterdam University Press/Van Gogh Museum Amsterdam; 2019. pp. 175-205

[36] Góra M, Targowski P, Kowalczyk A, Marczak J, Rycyk A. Fast spectral optical coherence tomography for monitoring of varnish ablation process. In: Castilleo M, Moreno P, Oujja M, Radvan R, Ruiz J, editors. Lasers in the Conservation of Artworks Proceedings of the International Conference Lacona VII,

Madrid, Spain, 17-21 September 2007. London: CRC Press, Taylor & Francis Group; 2008. pp. 23-27

[37] Targowski P, Marczak J, Kwiatkowska EA, Sylwestrzak M, Sarzyński A. Optical coherence tomography for high resolution real-time varnish ablation monitoring. In: Saunders D, Strlič M, Korenberg C, Luxford N, Birkhölzer K, editors. Lasers in the Conservation of Artworks IX Proceedings of the International Conference on Lasers in the Conservation of Artworks (Lacona IX), 7–10 September 2011, London, UK. London: Archetype Publications Ltd; 2013. pp. 26-31

[38] Iwanicka M, Musiela J, Łukaszewicz JW, Stoksik H, Sylwestrzak M. The potential of OCT for assessing laser assisted removal of deposits from ceramic tiles. In: Targowski P, Walczak M, Pouli P, editors. Lasers in the Conservation of Artworks XI, Proceedings of the International Conference LACONA XI, Kraków, Poland, 20–23 September 2016. Torun: NCU Press; 2017. pp. 105-114. DOI: 10.12775/3875-4.07

[39] Striova J, Salvadori B, Fontana R, Sansonetti A, Barucci M, Pampaloni E, et al. Optical and spectroscopic tools for evaluating Er:YAG laser removal of shellac varnish. Studies in Conservation. 2015;**60**(S1):S91-SS6. DOI: 10.1179/0039363015Z.000000000213

[40] Striova J, Fontana R, Barucci M, Felici A, Marconi E, Pampaloni E, et al. Optical devices provide unprecedented insights into the laser cleaning of calcium oxalate layers. Microchemical Journal. 2016;**124**:331-337. DOI: 10.1016/j.microc.2015.09.005

[41] Liang H, Lange R, Peric B, Spring M. Optimum spectral window for imaging of art with optical coherence tomography. Applied Physics B. 2013; **111**(4):589-602. DOI: 10.1007/s00340-013-5378-5

[42] Szkulmowski M, Tamborski S, Wojtkowski M. Spectrometer calibration for spectroscopic Fourier domain optical coherence tomography. Biomedical Optics Express. 2016;**7**(12): 5042-5054. DOI: 10.1364/boe.7.005042

[43] Sylwestrzak M, Szkulmowski M, Szlag D, Targowski P. Real-time imaging for spectral optical coherence tomography with massively parallel data processing. Photonics Letters of Poland. 2010;**2**(3):137-139. DOI: 10.4302/plp.2010.3.14

[44] Sylwestrzak M, Szlag D, Marchand PJ, Kumar AS, Lasser T. Massively parallel data processing for quantitative total flow imaging with optical coherence microscopy and tomography. Computer Physics Communications. 2017;**217**(Supplement C:128-137. DOI: https://doi.org/10.1016/j.cpc.2017.03.008

[45] de la Rie ER. The influence of varnishes on the appearance of paintings. Studies in Conservation. 1987; **32**:1-13. DOI: 10.2307/1506186

[46] Feller RL, Stolow N, Jones EH, editors. On Picture Varnishes and their Solvents. Revised and Enlarged Ed. Seminar on Resinous Surface Coatings; 1957. National Gallery of Art: Oberlin, Ohio; 1985

[47] Iwanicka M, Tymińska-Widmer L, Rouba B, Kwiatkowska EA, Sylwestrzak M, Targowski P. Through-glass structural examination of Hinterglasmalerei by optical coherence tomography. In: Radvan R, Asmus JF, Castillejo M, Pouli P, Nevin A, editors. Lasers in the Conservation of Artworks VIII Proceedings of the International Conference on Lasers in the Conservation of Artworks (Lacona VIII), 21-25 September 2009, Sibiu, Romania. London: CRC Press, Taylor & Francis Group; 2011. pp. 209-214